

Aeromagnetic Mapping of Basement Depth and Structure of the Calabar Flank and Adjoining Areas Southeastern Nigeria

G. E. Inyang¹, A. I. Opara¹, D. O. Ikoru¹, C. N. Okereke¹, C. P. Onyenegecha², E. M. Okoro^{3*}, A. I. Omenikolo⁴, I. A. Oha³ and J. N. Odi⁴

¹ Department of Geosciences, Federal University of Technology Owerri, Imo State, Nigeria

² Department of Physics, Federal University of Technology Owerri, Imo State, Nigeria

³ Department of Geology, University of Nigeria Nsukka, Enugu State, Nigeria

⁴ Department of Physics, Federal Polytechnic Nekede, Imo State, Nigeria

Received January 18, 2025; Accepted April 9, 2025

Abstract

Analysis of high-resolution aeromagnetic data covering the Calabar Flank and adjoining areas southeastern Nigeria was carried out in this study to map the depth and structuration of the basement outlining the region. The aeromagnetic data was reduced to the equator (RTE), and then subjected to regional-residual isolation using the polynomial fitting method to obtain the residual magnetic intensity (RMI) data of the study area. The RMI data was further analyzed using edge enhancement techniques including first vertical derivative (FVD), tilt derivative (TDR), and total horizontal derivative to outline the boundaries of linear, sublinear, and subrounded to round-shaped causative geological bodies in the subsurface. Magnetic basement depth estimation was achieved using the spectral analysis (SA) method, while 2D forward modeling of selected profiles gave insights into the architectural geometry of the basement blocks beneath the study area. Aeromagnetic expressions of the Calabar Flank and adjoining areas showed alternations in high and low anomalies, replicating susceptibilities variations of different rocks that make up the underlying geology of the area. The structural filtering methods applied to the RMI data highlighted the contacts of linear, sublinear, rounded, and subrounded geological features interpreted to represent subsurface lineaments, the Eastern Basement Shield of Nigeria, and intrusive (dyke-like) bodies that were emplaced into the overlying Cretaceous stratigraphy following tectono-magmatic episodes that have impacted the area throughout its evolutionary stages. The SA results yielded two-depth source model, with shallow sources ranging in depth from 0.28 to 0.53 km, while deeper source ensembles ranged in depth between 1.29 to 8.68 km. The modeled profiles revealed undulating basement topography characterized by horst-graben morphology. Parts of the study area with high sediment thicknesses could be favorable for hydrocarbon exploration.

Keywords: Aeromagnetic mapping; Basement depth; Structure; Hydrocarbon exploration; Calabar Flank.

1. Introduction

The Calabar Flank and adjoining areas is located within the southeastern part of Nigeria between latitude 4°30' - 6°00' N and longitude 7°00' - 9° 0' E. It covers an area of about 27,225 km² (Fig. 1). Following the recent crude oil discovery in the Gongola arm of the Northern Benue Trough, there has been growing interests from industry operators and the academia to re-assess the potentials of the Calabar Flank and environs which is believed to hold considerable promises for new prospect opportunities that will add to Nigeria's dwindling hydrocarbon reserves like other Cretaceous sedimentary basins in the country (e.g., Anambra, Bida, Dahomey, and Sokoto, Basins). However, limited access to subsurface data (like legacy 2D/3D seismic and well log data) has hampered detailed understanding of the strati-structural framework and trapping mechanisms in most of the afore-mentioned frontier basins in Nigeria, including the Calabar Flank. The need therefore arises to deploy cost-effective geophysical

tools to unravel the basement geometry and gain additional insights into the petroleum prospectivity of the Calabar Flank and adjoining areas.

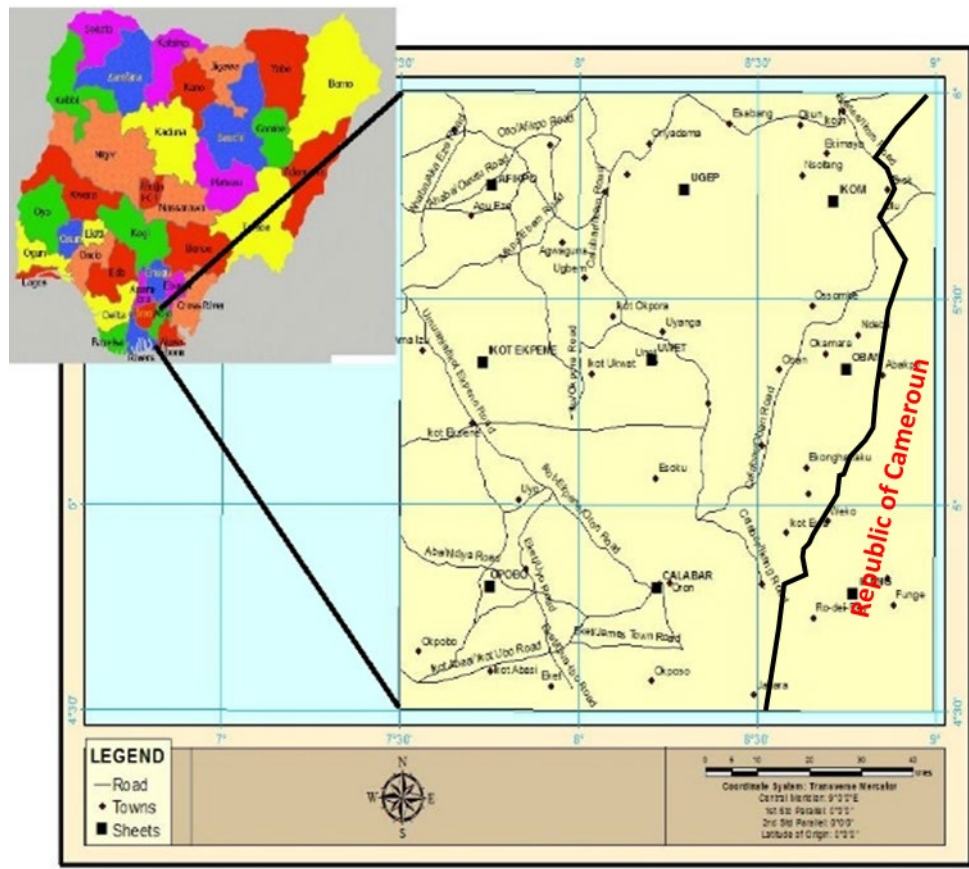


Fig. 1. Location map of the study area.

Aeromagnetic data is an invaluable geophysical tool utilized by geoscientists to map the extent, geometry, structure, depth, and morphology of the basement that underlies a sedimentary basin [1-2]. It is a fast and low-cost technique for regional evaluation of the hydrocarbon potential and solid mineral prospectivity of an area [3]. This geophysical method has been successfully deployed in different geological terrain to characterize the basement depth, and also determine the overlying stratigraphic thickness [4-6].

Several studies have been carried out to assess the petroleum potentials of the Calabar Flank and environs, using various geological and geophysical approach [7-10]. The present study aims at mapping the basement depth and structure of the Calabar Flank and adjoining areas within the southeastern part of Nigeria, using high-resolution aeromagnetic data. The study will shed light on the basement morphology and regional distribution of mini-basins which are potential sites for future hydrocarbon exploration campaign in the area.

2. Geologic setting

The Calabar Flank is a marginal/coastal sedimentary basin at the southeasternmost part of Nigeria, that developed following the Early Cretaceous rifting episodes associated with the separation of Africa from South American Plate [11-13]. According to [14], limits of the study area are defined by the Cameroun volcanic line (CVL) to the east, the Ikpe platform to the west, the Oban Massif to the north, and the Calabar Hinge Line to the south (Fig. 2). Tectonic elements in the area include the Oban Massif, Ituk High, and Ikang Trough, all juxtaposed into a horst-graben geometry that defines the underlying basement morphology (Fig. 3). The Calabar Flank is aligned in the NW – SE direction, orthogonal to the NE – SW trending Benue

megarift system, and extends beyond the Nigerian border into the southwestern part of Cameroon where it is delimited by the volcanic ridge [15-16].

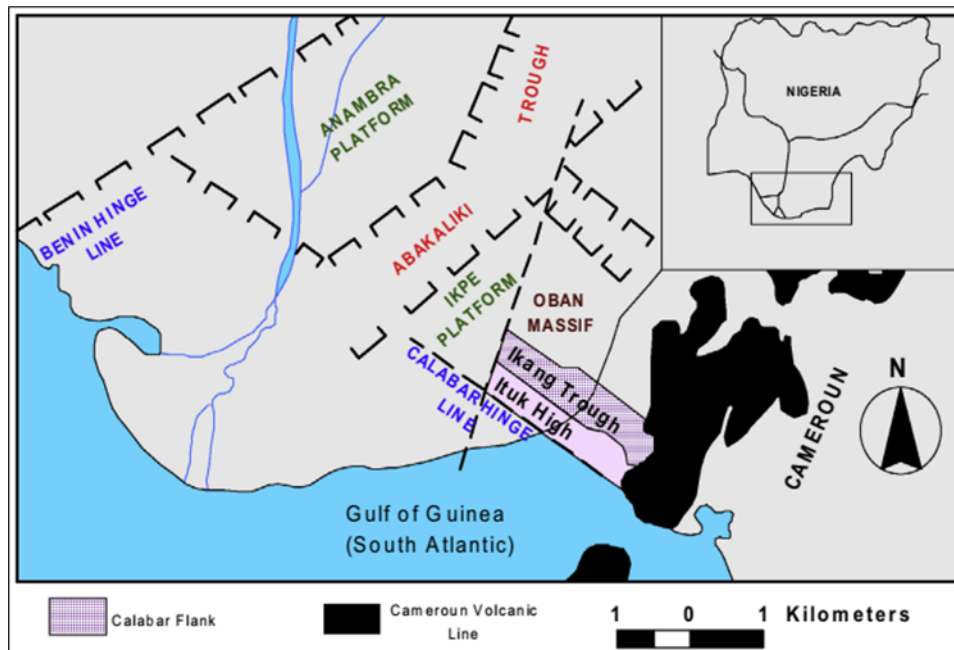


Fig. 2. Tectonic map of southern Nigeria showing the Calabar Flank and adjoining areas (modified after [14]).

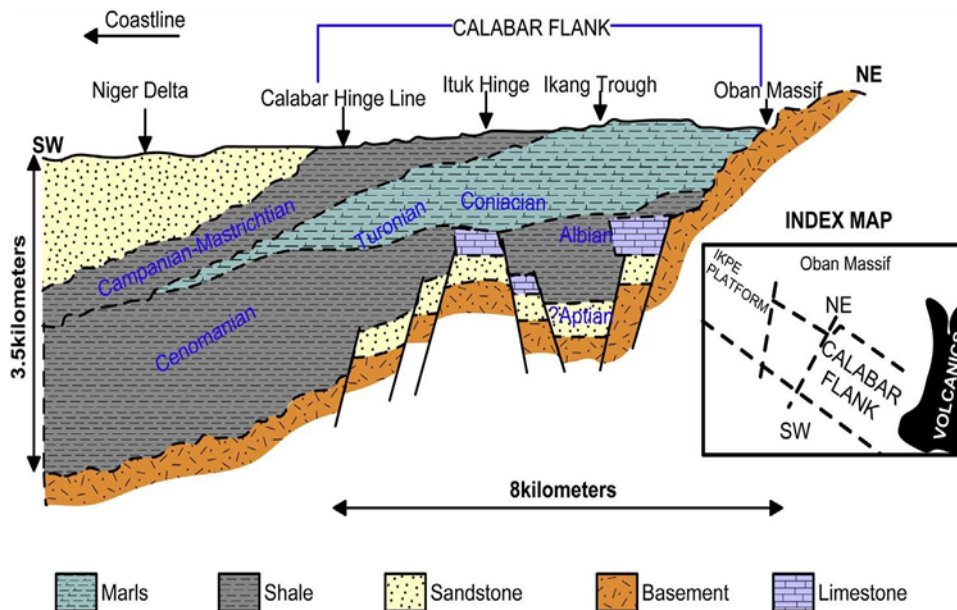


Fig. 3. Schematic representation of the horst-graben basement geometry beneath the Calabar Flank (modified after [14]).

Geological make-up of the study area includes the crystalline basement complex and sedimentary rocks. The Precambrian Basement Complex are essentially made up of granitic and magmatic rocks which exposed at the eastern portion of the area [17]. The Cretaceous - Tertiary sedimentary packages comprise of about 4 km thick sequences of alternating fluvial-continental, paralic, and marine sediments [18-19] (Fig. 4). The alternation of shale, sandstone and limestone sequences may indicate the presence of source rock facies, reservoirs, caprock and traps that make up the elements of a working petroleum system in the area.

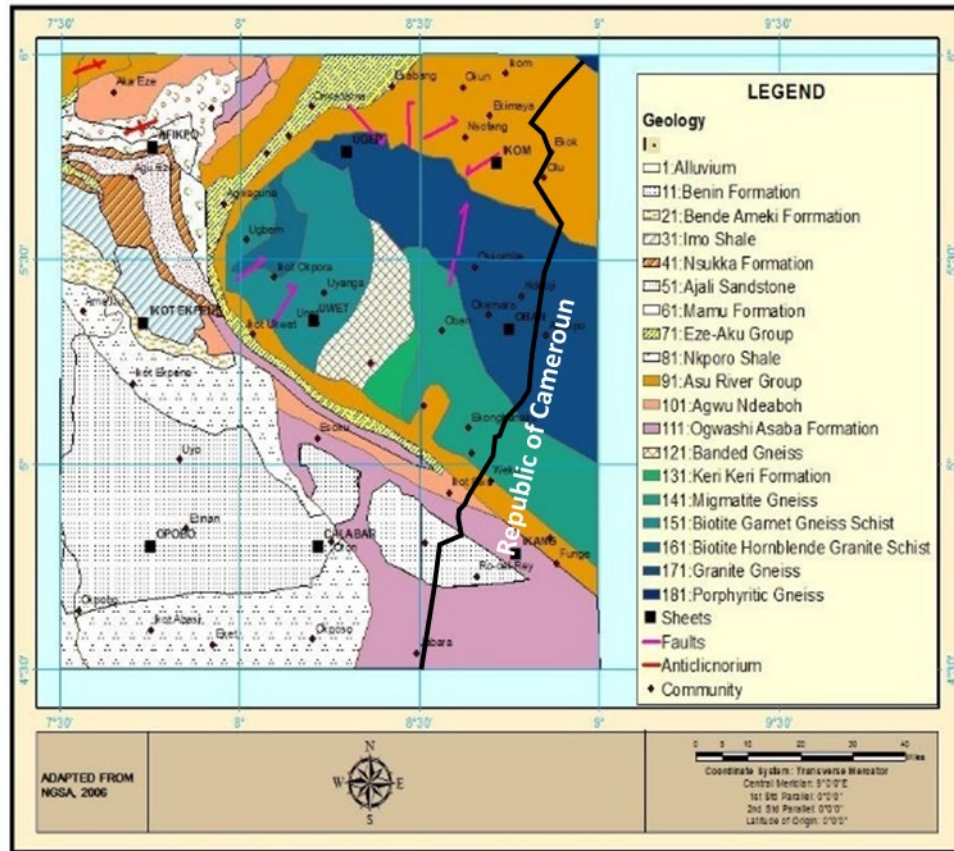


Fig. 4. Geological map of the study area (adapted from [33]).

The stratigraphic sequences of the Calabar Flank include the Aptian-Albian Awi Formation (fluvio-deltaic sandstones and grits) at the base, followed by the middle to late Albian Mfamosing Formation (limestone and calcareous sandstones. These are overlain by the intercalation of shales and limestones of the Cenomanian Odukpani Formation, the Coniacian Awgu Formation (shales and marls), and the Campano-Maastrichtian Nkporo Formation (carbonaceous shales) [20-21]. Sedimentation in the Calabar Flank were controlled by vertical motions along the fragmented basement blocks [19].

3. Materials and methods

3.1. Airborne magnetic data

The airborne magnetic data used in this study was obtained from the Nigerian Geological Survey Agency (NGSA). The data was acquired between the year 2003 and 2009 by Fugro for NGSA, as part of the nationwide aeromagnetic data acquisition geared towards enhancing solid mineral and hydrocarbon exploration in Nigeria. A total of nine (9) aeromagnetic data sheets covering the entire Calabar Flank and adjoining areas were merged into a single grid representing the total magnetic intensity (TMI) data of the study area (Fig. 5). The reduction to the equator (RTE) algorithm was applied to the TMI grid in order to remove anomaly inconsistencies and asymmetry associated with data acquired at low latitudes, thereby aligning the anomalies over the source bodies responsible for them [5]. The RTE grid of the study area (Fig. 6) was then subjected to region-residual isolation using the polynomial fitting method to obtain the residual magnetic intensity (RMI) grid, which formed the basis for further filtering techniques and interpretations carried out in this study.

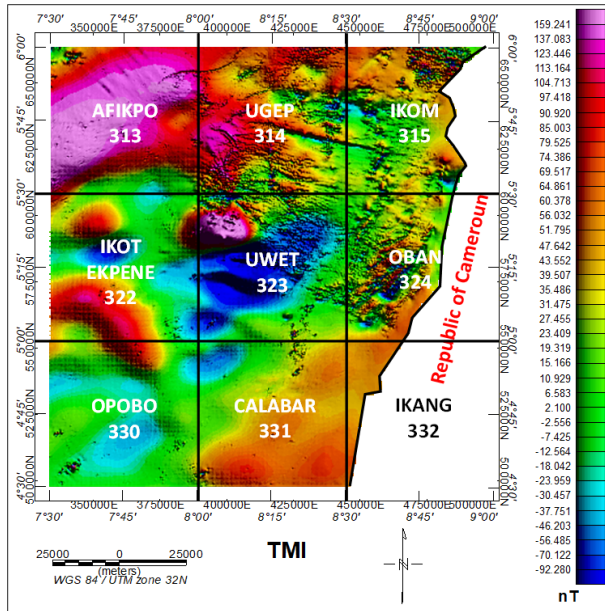


Fig. 5. Total magnetic intensity (TMI) map of the study area.

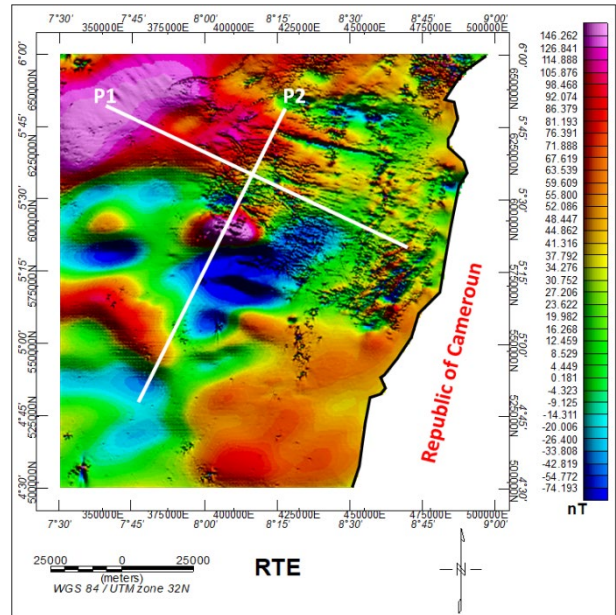


Fig. 6. Reduced to the equator (RTE) map of the study area showing the modeled 2D profiles.

3.2. Data processing and interpretation techniques

Structural enhancement filters including first vertical derivative (FVD), tilt derivative (TDR) and total horizontal derivative, were applied to the RMI data of the study area in order to highlight the boundaries and edges of subsurface geologic features in the area [22-25]. Analysis of the linear features interpreted from the filtered aeromagnetic data was done using rose diagram plots obtain the dominant tectonic trend in the study area. Estimation of magnetic basement depth was achieved using the spectral analysis method. 2D forward modeling of some selected profiles drawn on the RTE map was performed to understand the morphology and block pattern of the underlying basement rocks in the study area. Brief description of the methods used in this study is given below.

First vertical derivative (FVD)

The first vertical derivative filter accentuates short wavelength components of the magnetic anomaly field, while de-emphasizing long wave length components. It performs well in highlighting the details of anomaly texture, as well as the discontinuities and breaks in the anomaly pattern related to shallow laying geologic sources [23]. Mathematically, it is expressed as follows:

$$FVD = \frac{\partial F}{\partial Z} \quad (1)$$

Tilt derivative (TDR)

Tilt derivative (TDR) is a very good edge detection filter that highlights short wavelength anomalies, and enhances the presence of magnetic lineaments. [24] defined TDR as the ratio of the vertical derivative to the horizontal gradient of the potential field, expressed by the following equation:

$$TDR = \tan^{-1} \left(\frac{VDR}{THDR} \right) \quad (2)$$

TDR is a powerful tool for detecting the edges and contacts of near-surface geological features such as lineaments, fault, joints, and fractures because of its ability to emphasize both weak and strong magnetic anomalies.

Total Horizontal Derivative (THDR)

The total horizontal derivative of the magnetic data is a useful filter for delineating the boundaries of linear to sublinear causative bodies in areas of low magnetic gradients. This

filter enables easy mapping of shallow seated basement structures and mineral exploration targets. This method has a unique advantage over the other edge detectors in that it responds equally to shallow and deep sources [26]. The THDR is defined as:

$$TDHR = \sqrt{\left(\frac{\partial M}{\partial x}\right)^2 + \left(\frac{\partial M}{\partial y}\right)^2} \quad (3)$$

where $(\partial M/\partial x)$ and $(\partial M/\partial y)$ are the horizontal derivatives of the magnetic field.

Spectral analysis (SA)

Basically, the spectral analysis method considers the integral of the potential field at the surface from all depths, using the Fast Fourier Transform (FFT). The 2D power curve obtained from FFT filtering of the magnetic field data can yield the average depths to causative bodies in the subsurface. [27] defined the complex form of the 2D FFT pair as follows:

$$G(u, v) = \iint_{-\infty}^{\infty} g(x, y) e^{i(u_x - v_y)} d_x d_y \quad (4)$$

$$G(x, y) = \frac{1}{4\pi^2} \int_{-\infty}^{\infty} g(u, v) e^{i(u_x - v_y)} d_x d_y \quad (5)$$

where u and v are the angular frequencies in x and y directions respectively.

$G(u, v)$ can be divided into real and imaginary parts using the following equation:

$$G(u, v) = P(u, v) + iQ(u, v) \quad (6)$$

Then, the energy spectrum is expressed as,

$$E(u, v) = [G(u, v)]^2 = (P^2 + Q^2) \quad (7)$$

According to Spector and Grant [28] showed that the energy spectrum can be expressed in polar form as follows:

if $r^2 = (u^2 + v^2)$ and $\theta = \text{arc tan}\left(\frac{u}{v}\right)$, the energy spectrum $E(r, \theta)$ could be given by:

$$(E(r, \theta)) = 4\pi^2 M^2 R_G^2 (e^{-2hr}) ((1 - e^{-tr})^2) (S^2(r, \theta)) (R_p^2(\theta)) \quad (8)$$

where $\langle E(r, \theta) \rangle$ is the expected value; $r^2 = (u^2 + v^2)$ is the magnitude of the frequency vector; and $\theta = \text{arc tan}\left(\frac{u}{v}\right)$ is the direction of the frequency vector; M = magnitude of the moment/unit depth; h = the depth to top of the prism; t = the thickness to top of the prism; S = the factor for the horizontal size of the prism; R_p = the factor for the magnetization of the prism; R_G = the factor for geomagnetic field direction.

The average depth h to the ensemble can be estimated by the factor:

$$\{e^{-2hr}\} = \frac{e^{2hr} \sinh(2r\Delta h)}{4r\Delta t} \quad (9)$$

The energy spectrum will then consist of two parts: (i) the low frequency segment which decays rapidly and is associated with the deeper magnetic sources, and (ii) the high frequency segment which is related to shallower magnetic sources. Straight line slopes can be fitted to the 2D power curve to approximate the depths of the possible layers [28]. [29] have shown that the average depth to magnetic sources can be determined using the following empirical relations:

$$h(f) = \frac{M}{4\pi} M \times 0.08 \text{ cycles/unit distance} \quad (10)$$

$$h(f) = \frac{M}{2} M \times 0.5 \text{ radians/unit distance} \quad (11)$$

where $M = \frac{\text{Log } E}{f}$ is the gradient; $E(f) = e^{-2hf}$ is the energy spectrum, and $\text{Log } E$ is the variation of the logarithm of the power spectrum in the interval of frequency.

In this study, the spectral analysis procedure described above was used to estimate the depths to magnetic sources in the area. The RMI data was sub-divided into 31 blocks which were analyzed to obtain the 2D power curves using the FFT technique. Straight-line slopes were drawn to the obtained radial average power spectrum of each of the blocks to calculate the depth to magnetic basement in the Calabar Flank and adjoining areas.

4. Results and discussion

4.1. Magnetic expressions of the study area

The residual magnetic intensity (RMI) map of the study area (Fig. 7) revealed alternations in high (red), intermediate (green) and low (blue) magnetic anomalies, depicting susceptibility contrasts of the different rocks comprising the underlying geology of the Calabar Flank and environs. Major trends of the anomalies are in the NE – SW, NW – SE, E – W, and N – S directions. The anomalies range from -85.775 nT to 85.795 nT, with high magnetic signatures dominating the eastern, northeastern, central, parts of northwestern and southwestern portions of the area. Parts of the central and extreme northwestern portions of the study area are characterized by low magnetic anomalies, while intermediate magnetic signatures can be observed in almost every part of the RMI map.

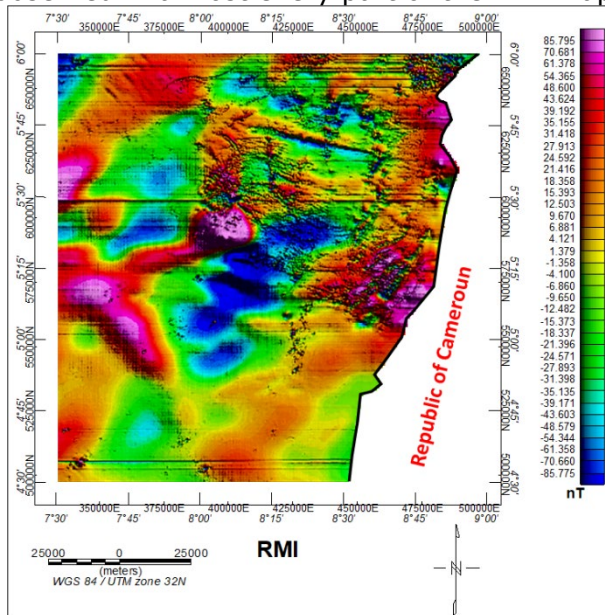


Fig. 7. Residual magnetic intensity (RMI) map of the study area.

The magnetic expression of the area observed on the RMI map showed good correlation with the subsurface geology displayed in figure 4. For instance, the trend of the high anomalies at the central and eastern parts of the study area followed the outline of the Oban Massif which forms one of the main tectonic elements in the Calabar region. Furthermore, the trend of the low anomaly zones towards the northwestern and southern portions of the study area mimics the outline of the Afikpo Syncline and Calabar Flank, respectively. In addition, low magnetic values generally reflect zones of low magnetization, while the areas with high magnetic values are indicates high magnetization. This implies that parts of the study areas characterized by high anomalies may be associated with intense tectonic/magmatic activities. Similarly, the several clusters of circular anomaly closures

with varying amplitudes observed at the northeastern end of the area may represent lithological variations of mafic - ultramafic intrusions within grano-dioritic batholiths [30-32]. In general, the anomalies showed sharp magnetic gradients, depicting signatures emanating from vertically inclined features.

4.2. Structural characteristics of the study area

The FVD and TDR maps of the study area (Fig. 8a&b) revealed variations in positive and negative magnetic anomalies that delineated the edges and boundaries of linear geological features. A NW – SE trending zone of high magnetic values occupying the central to eastern parts of the maps can be readily observed to follow the outline of the Oban Massif. This zone is characterized by NE – SW and NW – SE oriented anomalies that followed linear geological features like lineaments, fractures, joints, and faults that may have been developed following different episodes of intense tectono-magmatic activities that have impacted the basement rocks within the region over time. Towards the western and southern parts of the maps, the intensity of the linear anomalies deepens. This indicates that these parts of the study area are mainly underlain by sedimentary rocks, with lesser impacts from tectonic activities.

The FVD and TDR maps highlighted near-surface lineaments with major trends in the NE - SW, NW – SE, E – W, and N – S directions, as shown from the rose diagram plots (Fig. 8c&d). Towards the western and southern parts of the study area, high gradient FVD anomalies were interpreted to represent shallow seated basic igneous intrusions, while the low gradient FVD

anomalies represented metamorphically altered igneous intrusions. The prevalence of lineaments in the exposed basement areas is an indication that these geological features may have served as conduits through which hot molten magma ascended from deep inside the earth, and later solidified to form the exposed basement rocks. On the other hand, positive TDR values indicate a positive contrast of the causative sources while negative values are outside the source limits. The TDR also delineated NW – SE trending lineaments along the eastern part, and NE - SW oriented lineaments in northern and southern portions of the study area. These structural features formed the boundaries of horst and graben features of the basement blocks.

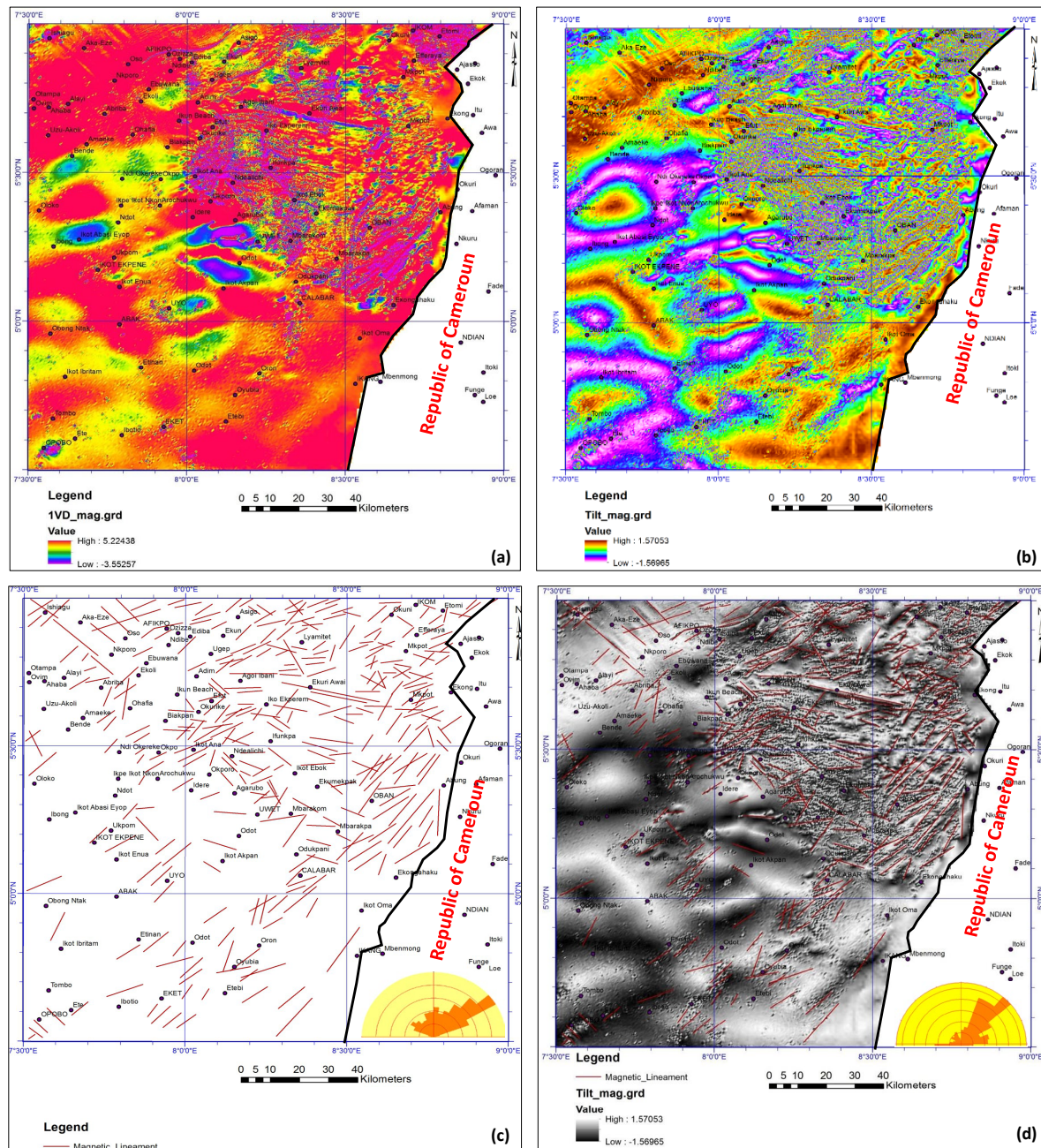


Fig. 8. Edge enhancement maps of the study area, with the interpreted lineaments and rose diagram plots. (a) FVD, (b) TDR, (c) FVD lineaments, and (d) TDR lineaments.

The THDR map (Fig. 9) delineated revealed prominent NE – SW and NW – SE trending high amplitude zones in the central, eastern and northeastern parts of the study area, interpreted

to represent the Eastern Nigerian Basement Complex (Oban Massif) and intrusive rocks beneath the study area. The boundaries of these anomalies coincided with the edges of known geological features within the Calabar Flank and adjoining areas. Zones characterized by low THDR anomalies indicate areas underlain by sedimentary rocks.

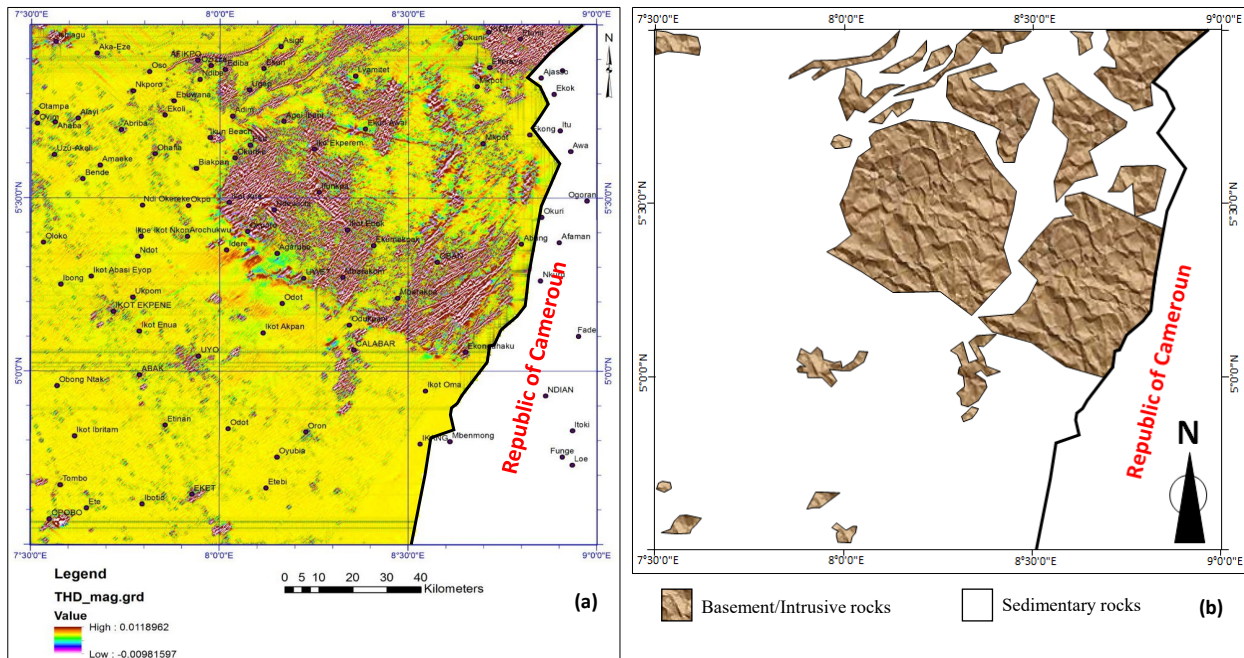


Fig. 9. (a) Total horizontal derivative (THDR) map, and (b) delineated intrusives and basement rocks in the study area.

4.3. Magnetic basement depth and block geometry

The obtained radially averaged power spectrum of the analyzed spectral blocks (Fig. 10) revealed a two-depth source model, representing depths to shallow (D1) and deep (D2) magnetic sources in the study area (Fig. 11). The estimated depths to shallow seated causative bodies in the study area range from 0.28 km to 0.53 km, with an average of 0.37 km (Table 1). These depths were interpreted to represent the magnetic effects of post Cretaceous intrusions emplaced within the sedimentary sequences overlying basement. The shallow depths may also indicate rock magnetizations emanating from near-surface ferruginous sandstones and ironstones that occur within the sediments.

The obtained depths to deeper basement sources in the study area ranged from 1.29 km to 8.68 km, with an average of 4.31 km. Spectral blocks covering the Ikom, Afikpo, Opobo, Calabar, and Iking regions revealed sedimentary thicknesses greater than 4 km. It is inferred that these parts of the study area have the thickest Cretaceous sedimentary successions. The estimated average depth to basement for deeper magnetic sources (D2) is adjudged in this study as the average depth to basement in the Calabar Flank and adjoining areas. Since sedimentary thicknesses are expected to increase as we move southwards towards the Atlantic and decrease as we move eastwards towards the Oban Massif, the depth values obtained in this study is therefore logical.

2D forward modeling of two selected profiles drawn across the RTE map revealed that the underlying basement rocks are characterized by a horst-graben geometry, depicting the variations in high and low magnetic anomalies on the RTE map of the study area (Fig. 12). As such, high anomaly zones indicated areas underlain by magnetite-rich rocks like the crystalline basement. Low anomaly zones suggested the prevalence sedimentary rocks with low magnetite content. Thus, basement the block pattern reflected a rugged topography, controlled by block faulting, vertical block movements, and block rotation. These processes exerted a major

influence on the overall framework of the overlying stratigraphy, and subsequent distribution of petroleum systems elements included source rocks, reservoir and seal facies, as well as the trapping mechanisms in the study area.

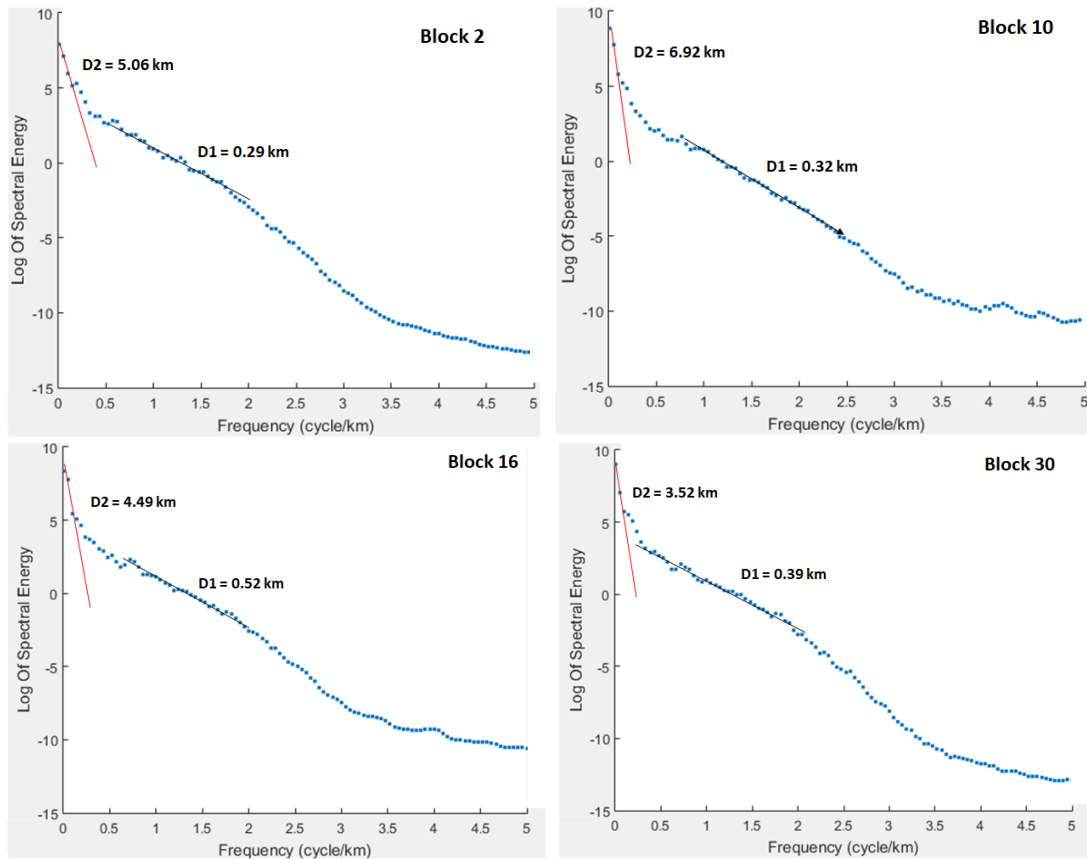


Fig. 10. Radially averaged power spectrum curves for Blocks 2, 10, 16, and 30.

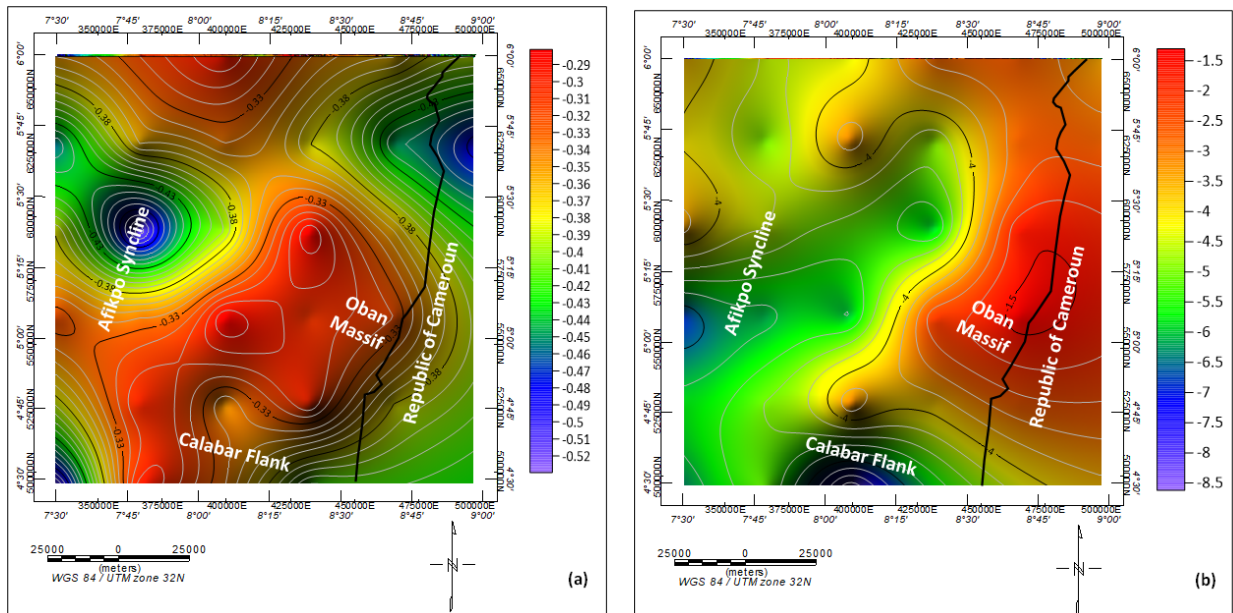


Fig.11. (a) Depth map of shallow basement sources (D1). (b) Depth map of deeper basement sources.

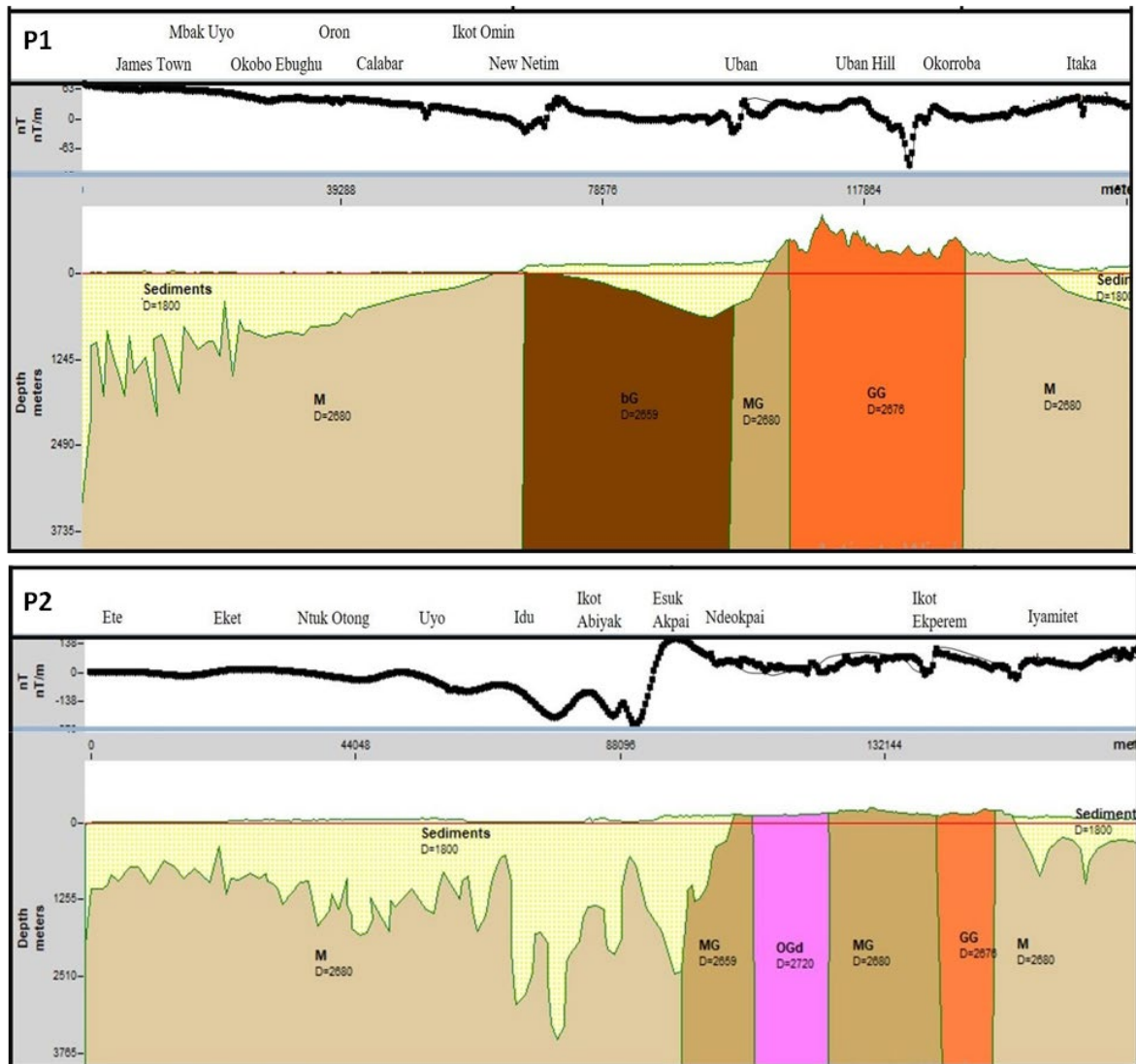


Fig. 12. Profiles 1 and 2 showing the block geometry and horst-graben morphology of the basement beneath the Calabar Flank and adjoining areas.

5. Conclusion

The interpretation of high-resolution aeromagnetic data covering the Calabar Flank and adjoining areas, southeastern Nigeria have been attempted in this study, with the view to establish the basement depth and structure of the region. The obtained TMI, RTE, and RMI maps revealed that the area is characterized by variations in high, low, and intermediate magnetic anomalies reflecting the varying susceptibilities in the rocks that constitute the overall geologic make-up of the region. The enhanced magnetic maps generated by applying FVD, TDR, and THDR filters to the RMI data highlighted the edges and boundaries of lineaments, basement, and intrusions emplaced with the sedimentary successions in the area. Major orientation of these geological features is in the NE – SW, NW – SE, E – W, and N -S directions. The estimated average depth to basement of 4.31 km suggests that the area might be prospective for hydrocarbon exploration, since the sediments thickens towards the southern and western parts of the study area covered by the Calabar Flank and Afikpo Syncline. However, the preponderance of lineaments towards the eastern and northeastern parts covered by the Oban Massif at an average shallow depth of 0.37 km is a clear indication that the area might be favorable for ore mineral exploration.

Acknowledgements

This study was funded 100% by Tertiary Education Trust Fund National Research Fund (TETFUND NRF), Nigeria via the 2021 National Research Fund grant cycle with grant number: TETF/ES/DR&D-CE/NRF2021/SETI/GEO/00038/VOL. 1. The authors are also grateful to the management and staff at the Nigerian Geological Survey Agency (NGSA) and the Federal University of Technology Owerri for their technical and data support.

References

- [1] Gunn PJ. Application of aeromagnetic surveys to sedimentary basin studies" AGSO Journal of Australian Geology and Geophysics, 1997; 17(2):133-144.
- [2] Aitken ARA, Betts PG. (2009). Multi-scale integrated structural and aeromagnetic analysis to guide tectonic models: An example from the eastern Musgrave Province, Central Australia. *Tectonophysics*, 2009; 476, 3-4: 418-435.
- [3] Omenikolo IA, Opara AI, Okereke CN, Ikoro DO, Emberga TT, Agoha CC, Nwokeabia CN. Spectral Depth Estimation of the Magnetic Basement in Parts of the Benue Trough Using High-Resolution Aeromagnetic Data: Implication for Hydrocarbon Prospectivity. *Pet. Coal*, 2023; 65(1): 138-152.
- [4] Airo M, Loukola-Ruskeeniemi K. Characterization of sulfide deposits by airborne magnetic and gamma-ray responses in eastern Finland. *Ore Geology Reviews*, 2003; 24: 67-84.
- [5] Okoro EM, Onuoha KM, Oha AI. Aeromagnetic interpretation of basement structure and architecture of the Dahomey Basin, Southwestern Nigeria. *NRIAG J Astron Geophys*, 2021; 10(1):93-109
- [6] Ekwok SE, Akpan AE, Achadu OM, Eze OE. Structural and lithological interpretation of aerogeophysical data in parts of the Lower Benue Trough and Obudu Plateau, Southeast Nigeria. *Advances in Space Research*, 2021; <https://doi.org/10.1016/j.asr.2021.05.019>
- [7] Odumodu CF. Temperatures and Geothermal Gradient Fields in the Calabar Flank and Parts of the Niger Delta, Nigeria. *Petroleum Technology Development Journal*, 2012; 2:1 - 17.
- [8] Boboye OA, Okon EE. Sedimentological and geochemical characterization of the Cretaceous strata of Calabar Flank, southeastern Nigeria. *Journal of African Earth Sciences*, 2014; 99: 427-441.
- [9] Opara AI, Onyewuchi RA, Selemo AOI, Onyekuru SO, Ubechu BO, Emberga TT, Ibim DF, Nosiri OP. (2014.). Structural and tectonic features of Ugep and Environs, Calabar Flank, South-eastern Nigeria: Evidences from aeromagnetic and Landsat-ETM data. *Mitteilungen Klosterneuburg*, 2014; 64(7): 33-54.
- [10] Ekwok SE, Akpan AE, Achadu O-IM, Thompson CE, Eldosouky AM, Abdelrahman K, Andr  s P. Towards Understanding the Source of Brine Mineralization in Southeast Nigeria: Evidence from High-Resolution Airborne Magnetic and Gravity Data. *Minerals*, 2022; 12:146. <https://doi.org/10.3390/min12020146>
- [11] Burke KC, Dessauvagie RFJ, Whiteman AW. Geological history of the Benue valley and adjacent areas. In: Dessauvagie TFJ, Whiteman AJ (eds). *African Geology*, University of Ibadan Press, 1972;187-206
- [12] Benkheilil J. Cretaceous deformation, magmatism and metamorphism in the lower Benue Trough, Nigeria. *Geo J.*, 1987; 22: 467-493.
- [13] Reijers TJA, Petters SW. Sequence Stratigraphy Based on Microfacies Analysis: Mfamosing Limestone, Calabar Flank, Nigeria. *Geologie en Mijnbouw*, 1997; 76(3):197-215.
- [14] Nyong EE, Ramanathan RA. Record of Oxygen deficient paleoenvironments in the Calabar Flank, S.E. Nigeria. *Journal of African Earth Sciences*. 1985; 3(4):455-460.
- [15] Reymont RA. Aspects of the Geology of Nigeria, Ibadan University. Press, Ibadan, 445.
- [16] Schmidt, E. 1972. Operating instructions: Concrete test hammer N. Consulting Engineer, Bachlettenstrasse, 52, CH-400. Basle, Switzerland.
- [17] Zaborski PM. A Review of the Cretaceous System in Stratigraphy. *Palaeotographica (A)*, 1998; 179: 1-104.
- [18] Ofoegbu CO, Onuoha KM. Analysis of magnetic data over the Abakaliki Anticlinorium of the Lower Benue Trough. Nigeria, *Marine and Petroleum geology*, 1991; 8: 174.
- [19] Edet JJ and Nyong EE. Depositional environments, sea-level history and palaeobiogeography of the late Campanian-Maastrichtian on the Calabar Flank, Southeastern Nigeria. *Palaeoecology*. 1993; 102: 161-175.
- [19] Boboye OA, Oyeyipo AD. Geochemical Appraisal of Ekenkpon Shale in the Calabar Flank, Southeastern Nigeria. *Pet. Coal*, 2017; 59(1): 122-134.

- [20] Adeleye DR, Fayose EA. Stratigraphy of the type section of Awi Formation, Odukpani area, southeastern Nigeria. *Journal of Mining and Geology*, 1978; 15: 33-37.
- [21] Petters SW. Central West African Cretaceous Tertiary benthic foraminifera and Stratigraphy. *Palaeotographical (A)*, 1982; 179:1-104.
- [22] Blakely RJ. Potential theory in gravity and magnetic applications. Cambridge 757 University Press, 1995; 81- 87. <https://doi.org/10.1017/CB09780511549816>
- [23] Milligan PR, Gunn PJ. Enhancement and presentation of airborne geophysical data. *AGSO J Aust Geol Geophys.*, 1997; 17(2): 63-75.
- [24] Verduzco B, Fairhead JD, Green CM, MacKenzie C. New insights into magnetic derivatives for structural mapping. *The Leading Edge*, 2004; 23(2):116-119. <https://doi.org/10.1190/1.1651454>
- [25] Nabighian MN, Grauch VJS, Hansen RO, LaFehr TR, Li Y, Peirce JW, Philips JD, Ruder ME. The historical development of the magnetic method in exploration. *Geophysics*, 2005; 33 – 61. <https://doi.org/10.1190/1.2133784>
- [26] Miller HG, Singh V. Potential field tilt-a new concept for location of potential field sources. *Journal of Applied Geophysics*, 1994; 32(2-3):213-217. [https://doi.org/10.1016/0926-9851\(94\)90022-1](https://doi.org/10.1016/0926-9851(94)90022-1)
- [27] Bhattacharyya BK. Continuous spectrum of the total magnetic field anomaly due to rectangular prismatic body. *Geophysics*, 1966; 31: 197 – 212. <http://dx.doi.org/10.1190/1.1439767>
- [28] Spector A, Grant FS. Statistical models for interpreting aeromagnetic data. *Geophysics*, 1970; 35 (2), 293-302. <https://doi.org/10.1190/1.1440092>
- [29] Hinze WJ, Von Frese RRB, Saad AH. Gravity and magnetic exploration principles, practices, and applications. Cambridge University Press, New York, 2013. <https://doi.org/10.1017/CB09780511843129>
- [30] Ghazala HH. Geological and structural interpretation of airborne surveys and its significance for mineralization, South Eastern Desert Egypt. *Journal of African Earth Sciences*, 1997; 16(3), 273-285.
- [31] Gupta VH, Ramani SD. Optimum second vertical derivative application in geologic mapping and mineral exploration. *Geophysics*, 1982; 24: 582-601.
- [32] Opara AI, Ugwu SA, Onyewuchi RA. Structural and Tectonic interpretations from Landsat Thematic Imagery: case study of Okposi Brine Lake and environs, Lower Benue Trough, Nigeria; *Elixir Remote Sensing*, 2012; 49: 9708-9713.
- [33] Nigerian Geological Survey Agency (NGSA). Geology and mineral resources of North Central Zone Nigeria, NGSA Regional geology and mineral series, 2008; 1: 1 - 29.

To whom correspondence should be addressed: E. M. Okoro, Department of Geology, University of Nigeria Nsukka, Enugu State, Nigeria, E-mail: ezemartok@gmail.com <https://orcid.org/0000-0002-8387-8489>